

PROBABILISTIC SEISMIC HAZARD ANALYSIS IN NEW ZEALAND USING PHYSICS-BASED GROUND MOTION SIMULATION METHODOLOGY

Karim TARBALI^{1,*}, Brendon BRADLEY¹, Jonney HUANG¹, Robin LEE¹, Daniel LAGRAVA¹, Sung BAE¹, Viktor POLAK¹, Jason MOTHA¹ & Melody ZHU¹

Abstract: *This paper presents the computational components and results of the May 2018 version (v18.5) of probabilistic seismic hazard analysis (PSHA) in New Zealand based on physics-based ground motion simulations ('Cybershake NZ'). A total of 11,362 finite fault simulations are undertaken and seismic hazard results are computed on a spatially-variable grid of 27,481 stations, with distributed seismicity sources considered via conventional empirical ground motion models. In the current work completed to date, the Graves and Pitarka (2010, 2015) hybrid broadband ground motion simulation approach is utilized considering a transition frequency of 0.25 Hz, a detailed crustal model with a grid spacing of 0.4 km, and an empirically-calibrated local site response model. A Monte Carlo scheme is used to sample variability in the seismic source parametrization (by varying the hypocentre location and slip distribution per each hypocentre realization), with the total number of ruptures for each fault being a function of the rupture magnitude. The generated uniform hazard maps across the country are presented. Treatment of uncertainty in the context of simulation-based PSHA and improvements for future versions of the ongoing effort are discussed.*

Introduction

Probabilistic seismic hazard analysis (PSHA) is a key component in seismic design and performance assessment of engineered systems, which considers the likelihood of possible earthquake scenarios in the region of interest using an earthquake rupture forecast (ERF) and combines it with the estimates of exceedance probability for given ground motion levels using a ground motion model (GMM). Accurate representations of rupture characteristics, wave propagation, and subsurface soil behaviour are necessary for PSHA. Conventionally, simplified models are used to estimate resulting ground motions (utilizing empirical GMMs), which neglects the inherent physical complexities in earthquake rupture and ground motion properties, such as slip heterogeneity, rupture directivity, and basin depth and edge effects, among others. In addition, issues such as the paucity of ground motions recorded from large magnitude ruptures in the near-fault region, assumptions regarding the ergodicity in ground motion properties for a given site subjected to a given earthquake, and the significant epistemic uncertainty in using empirical GMMs (Bommer *et al.*, 2005, 2010; Strasser, Abrahamson and Bommer, 2009) motivates utilizing alternative GMMs for seismic hazard analysis. Validation of simulated ground motions against the observed ground motions from the past events (e.g., Taborda and Bielak, 2013; Goulet *et al.*, 2015; Graves and Pitarka, 2015; Taborda *et al.*, 2016; Bradley, Razafindrakoto and Polak, 2017; Razafindrakoto, Bradley and Graves, 2018) demonstrates the capabilities of simulations to be used for seismic hazard analyses, such as through the 'Cybershake' project in California (Graves *et al.*, 2011; Callaghan *et al.*, 2017).

This paper presents the computational components and preliminary results from version 18.5 of utilizing physics-based ground motion simulation approach for seismic hazard analysis in New Zealand (Cybershake NZ v18.5). In the following sections, the

¹ University of Canterbury and New Zealand Centre for Earthquake Resilience (QuakeCoRE), Christchurch, New Zealand.

* Postdoctoral Fellow, karim.tarbali.p@gmail.com

corresponding computational components are discussed and illustrative results from the conducted analyses are presented with contextual discussion.

Computational workflow

Cybershake NZ v18.5 considers different approaches for calculating the hazard from finite faults and distributed seismicity sources of Stirling et al. (2012), as presented in Figure 1. Comprehensive physics-based ground motion simulations are used to characterize ground motion distributions from realizations of finite-fault ruptures, whereas empirical GMMs are utilized for the distributed seismicity sources due to the significant uncertainty in their geometry and rupture parameters. As the distributed seismicity source models improve in future, they can be included in the simulation branch of Figure 1 (mainly for regions where the seismic hazard is dominated by these sources). In the v18.5 execution, ground motions are simulated using the hybrid broadband simulation approach of Graves and Pitarka (2010, 2015) considering a transition frequency of 0.25 Hz, a detailed crustal model with a grid spacing of 0.4 km, a minimum shear wave velocity of 500 m/s, and the empirically-calibrated local site response model of Campbell and Bozorgnia (2014).

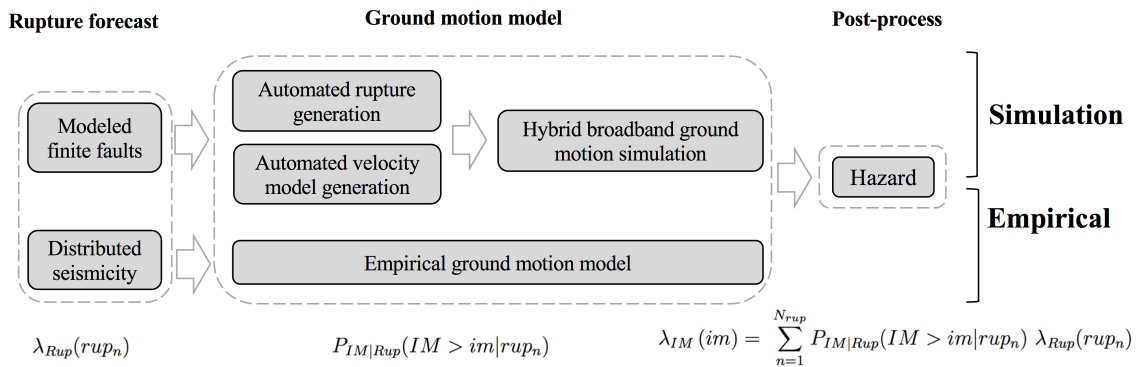


Figure 1: Computational workflow of Cybershake NZ v18.5. The physics-based ground motion simulation approach is utilized for kinematic rupture realizations of finite faults and empirical GMMs are used for distributed seismicity sources.

The present simulation-based PSHA of California via the SCEC Cybershake effort (Graves et al., 2011) utilizes reciprocity due to the larger number of considered sources (i.e., 415,000 rupture realizations) in comparison to the number of recording stations (250). In contrast, Cybershake NZ uses a forward simulation approach as the total number of finite faults in Stirling et al. (2012) (i.e., 536), and the resulting rupture realizations (i.e., 11,362 in the current version as elaborated on subsequently) are significantly less than the number of recording stations (27,481 in the current ground motion recording grid utilized). The significantly larger number of recording stations (27,481 vs. 250) is based on feedback as to the desired level of spatial resolution for simulation outputs for engineering application of simulated ground motions. The desire to directly use forward simulation is also based on the envisaged plans to implement a workflow that is future-proof to the inclusion of nonlinearities in ground motion simulation (Taborda, Bielak and Restrepo, 2012; Roten et al., 2017).

Kinematic rupture generation

The workflow presented in Figure 1 includes automated generation of kinematic ruptures based on Graves and Pitarka (2015) method considering the fault geometry, seismic moment, rake angle, and hypocentre location. Figure illustrates the 473 shallow-crustal faults of Stirling et al. (2012) considered in the current execution. Note that 47 offshore small-magnitude shallow-crustal faults with negligible contribution to the hazard, and the eight subduction sources are excluded. Note that subduction ruptures were excluded in

v18.5 as the ground motion simulation validation efforts (in New Zealand and elsewhere) have mostly focused on shallow-crustal events (Goulet *et al.*, 2015; Graves and Pitarka, 2015; Bradley, Razafindrakoto and Polak, 2017; Razafindrakoto, Bradley and Graves, 2018).

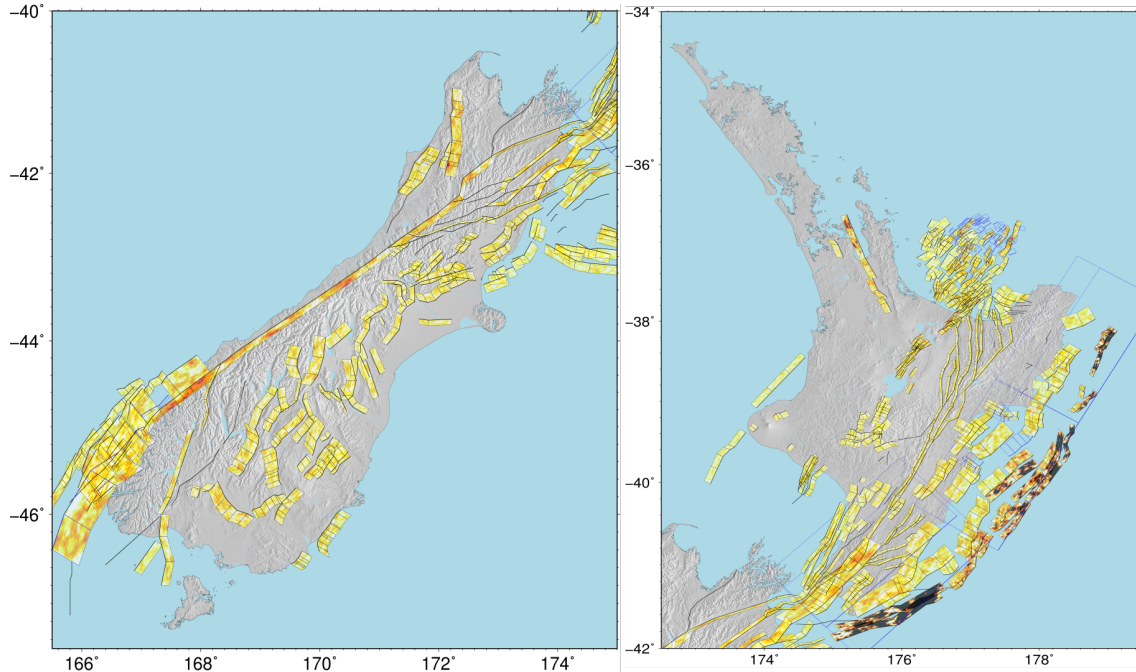


Figure 2: The 473 considered shallow-crustal finite faults in Cybershake NZ v18.5: (left-panel) South Island; (right-panel) North Island. The surface projection of the excluded 55 offshore small-magnitude shallow-crustal faults with negligible contribution to the hazard and 8 subduction faults are shown in blue.

Considering the utilization of distributed seismicity recordings to estimate the lower seismogenic depth of finite faults (Stirling *et al.* 2012) and past investigations regarding the occurrence of ruptures beyond the inferred depths (King and Wesnousky, 2007), ruptures with lower seismogenic depths of 12 km (or larger) in Stirling *et al.* (2012) are considered to extend 3km beyond the corresponding lower seismogenic depth. A similar approach was considered by Graves and Pitarka (2015) and is shown to alleviate the inconsistency in the long-period content of simulated ground motions in comparison to observations. Rupture moment magnitudes were calculated based on the Leonard (2010) relationship (considering the modification to their seismogenic depths).

A Monte Carlo scheme is used to sample variability in the seismic source parametrization by varying the hypocenter location based on Mai *et al.* (2005) and slip distribution per each hypocenter realization using the Graves and Pitarka (2015) rupture generator. The total number of realizations for a given fault was determined based on its corresponding rupture magnitude (as shown in

Figure 3). A minimum of 10 realizations are considered for faults with magnitudes smaller than 6. In total, 11,362 finite fault ground motion simulations were conducted.

Figure 3a presents the number of considered realizations and the core hours to conduct simulations on the Nesi Kupe skylake processors (~150,000 core hours in total) using optimized velocity model domains (as elaborated on in the next subsection) with 0.4 km grid size and varying total simulation durations.

Velocity model generation

The velocity model domain is generated specifically for each and every fault using an optimization algorithm which maximizes the land coverage of the simulation domain (in order to remove the unnecessary computational burden of simulating ground motions

offshore). The initial horizontal extents of the domain are calculated by computing a boundary around the fault that corresponds to a peak ground velocity (PGV) of 2 cm/s using the Bradley (2013) empirical GMM. This initial domain is rotated to align in its largest extent with the centre line of the country landmass. Then, if the domain boundaries extend offshore, the extents are reduced considering that the domain edges should be 15 km away from the fault edges and 5km away from the shoreline (whichever is the largest). A detailed velocity model of Lee et al. (2017) for the Canterbury region and Eberhart-Phillips et al. (2010) for the rest of New Zealand are utilized for generating velocity models.

Figure 3b presents this process for AlpineF2K fault, illustrating the initial and optimized domains. Note that the criteria utilized for the optimization are iteratively determined considering different rupture sizes and the shape of the country landmass. The depth of simulation velocity models is calculated considering the corresponding rupture magnitude and the minimum depth that enables capturing the downward radiated waves.

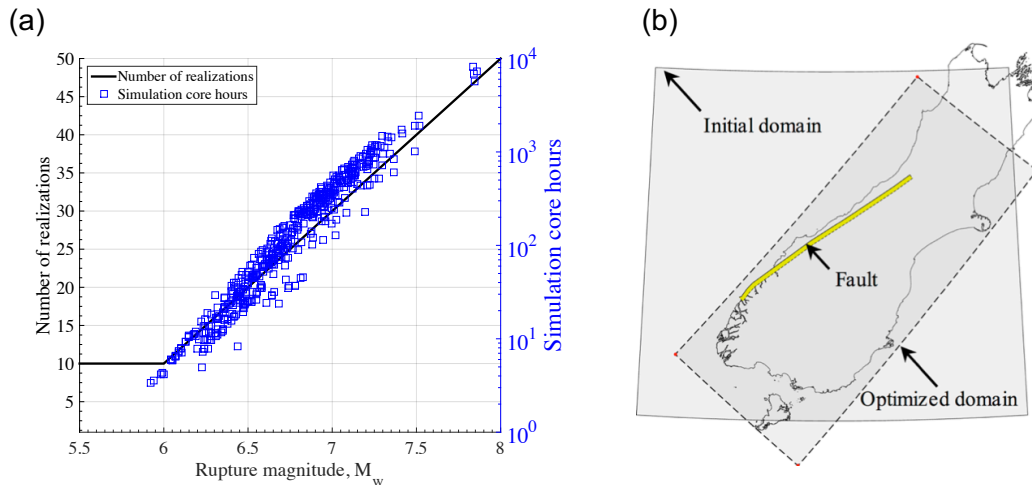


Figure 3: (a) The model utilized to determine the number of realizations based on the rupture magnitude for v18.5, and the corresponding core hours on the Nesi Kupe Skylake processors to conduct simulations using optimized velocity model domains. (b) Illustration of the automated velocity model generation and optimization of the land coverage for AlpineF2k fault as an example.

Ground motion recording grid and sub-surface site condition

In order to have a consistent grid of points on the surface to store the simulated ground motions and combine the results to obtain seismic hazard, a nation-wide grid of recording stations is generated (as shown in Figure 4a-b). This grid has a non-uniform spatial density which is a function of population density and sub-surface soil condition. The population data provides an appropriate constraint to have a coarser grid size in mountainous regions, and finer grid sizes in highly populated regions (which provides a robust means for site-specific PSHA). All the strong-motion stations of GeoNet (<https://github.com/GeoNet/delta>) are also included in the generated grid in order to provide a means to compare the simulated ground motions with those from future events (if the simulation assumptions are close to the corresponding rupture characteristics). Figure 4c-d present the time-averaged shear wave velocity in the top 30 m (V_{s30}) based on Foster et. al. (2019) (developed using surficial geology, topography, and direct measurements). The V_{s30} values are utilized by empirical GMMs, in addition to considering local site response for the simulated ground motions based on the Campbell and Bozorgnia (2014) model.

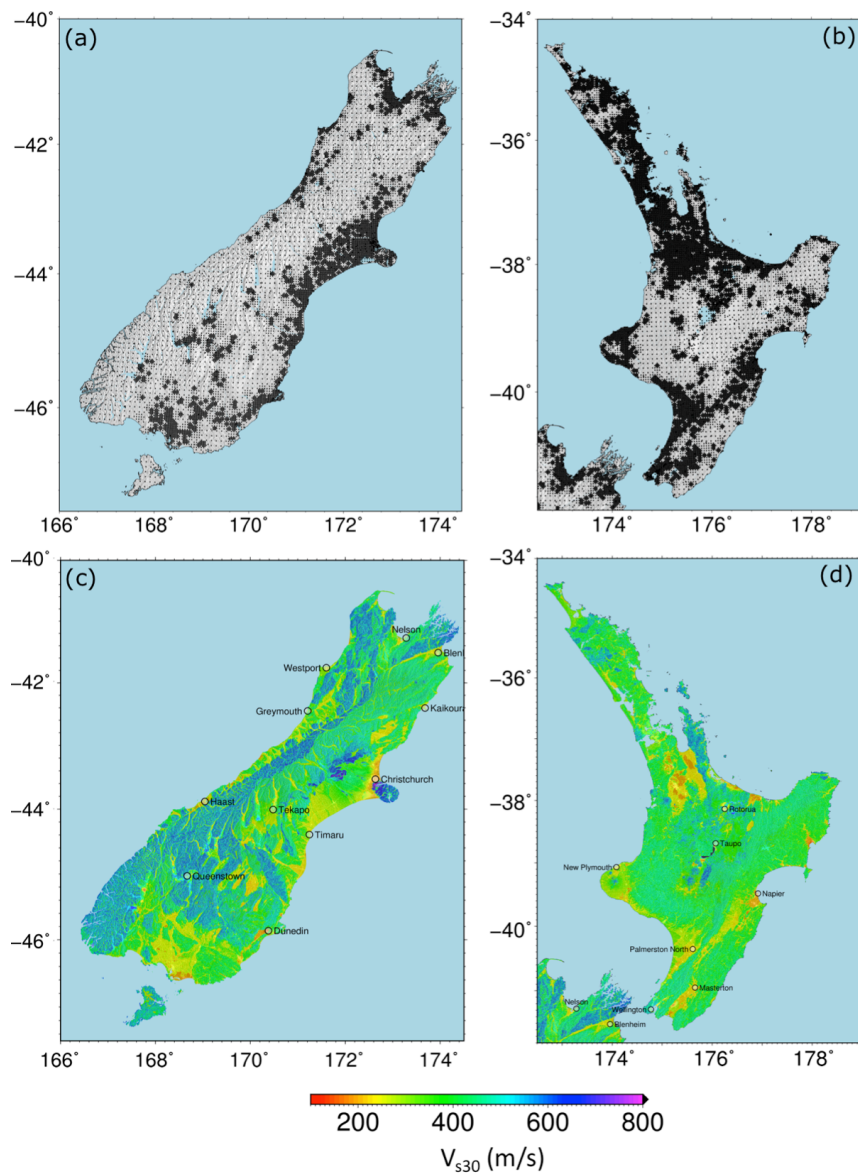


Figure 4 (a)-(b) A non-uniform grid with 27,481 sites generated based on population density and subsurface soil condition to extract simulated ground motions and perform PSHA; and (c)-(d) the corresponding time-averaged shear wave velocity in the top 30 m (V_{s30}) based on Foster et al. (2018).

Results

Figure 5a and 5d present the uniform-hazard ground motion map corresponding to the 10% in 50 years exceedance probability based on the Cybershake v18.5 results for the PGV and pseudo-spectral acceleration (pSA) for 5.0 s vibration period. Figures 5b and 5e present the counterpart results from the empirical GMM of Bradley (2013), and Figures 5c and 5f illustrate the natural logarithm of the Cybershake v18.5 over empirical ground motion ratios.

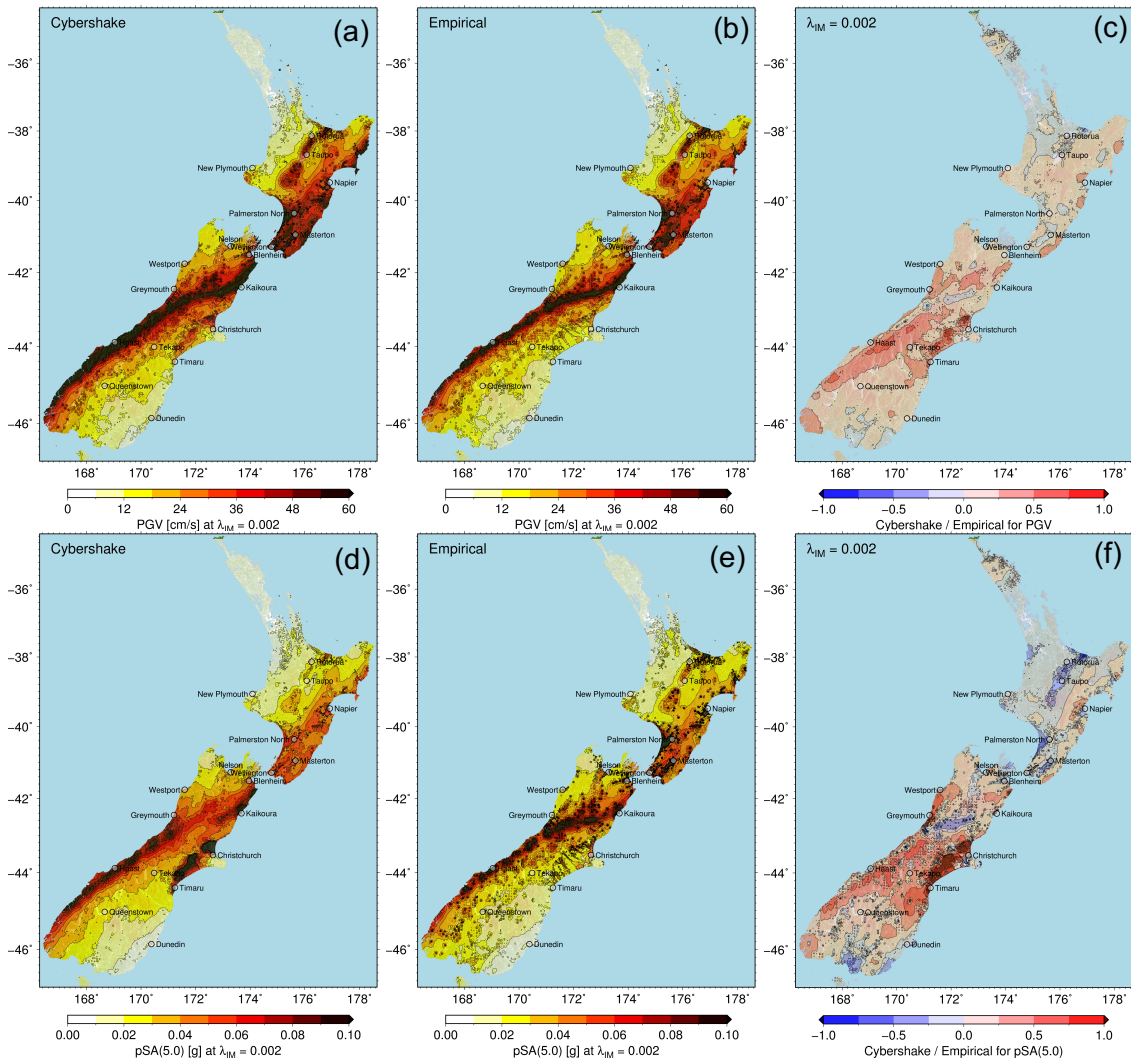


Figure 5: Uniform hazard ground motion map for the PGV and pSA (5.0 s) values corresponding to the 10% in 50 years hazard: (a) and (d) Cybershake v18.5; (b) and (e) empirical GMM of Bradley (2013); and (c) and (f) natural logarithm of Cybershake v18.5 over empirical ground motion ratios.

These results illustrate the differences between the two ground motion modelling approaches for different regions. It is noted that the PGV results are mainly contributed by the high-frequency portion of the simulated ground motions which is based on a phenomenological simplified physics approach (Boore, 1983; Graves and Pitarka, 2010), however, the pSA (5.0 s) values are mainly contributed by comprehensive physics-based simulations. The difference between the Cybershake and empirical approaches for pSA (5.0 s) is more pronounced for the Canterbury region which is located on a deep sedimentary basin (incorporated in the utilized velocity model). In addition to representing site-specific characteristics of hazard, another distinct difference between the Cybershake and empirical approaches in terms of application is the fact that the site-specific ground motion time series (produced by Cybershake simulations) can be utilized in seismic response analysis of engineered systems once appropriate confidence is built through further validation efforts (Bradley *et al.*, 2017). The future versions of Cybershake NZ will progressively aim to increase the transition frequency in order to

encompass higher frequency contents of ground motions within the comprehensive physics-based portion.

Discussion and conclusion

This paper presented the computational components and results of the May 2018 version (v18.5) of physics-based PSHA in New Zealand ('Cybershake NZ'). Cybershake NZ v18.5 and prior versions provided initial prototypes to refine the designed and implemented computational workflow (and its underlying components) to conduct Cybershake analyses in New Zealand. The Graves and Pitarka (2010, 2015) method was used in v18.5 to conduct ground motion simulations for the finite faults of Stirling *et al.* (2012) with a grid spacing of 0.4 km and a transition frequency of 0.25 Hz. A Monte Carlo scheme was used to sample variability in hypocentre location and slip distribution in Cybershake NZ v18.5 in order to partially account for ground motion variability. A total of 11,362 finite fault ground motion simulations are undertaken and seismic hazard results are extracted on a spatially-variable grid of 27,481 stations.

In order to obtain a more accurate characterization of the near-fault seismic hazard, a larger number of slip and hypocentre realizations (Graves *et al.*, 2011; Callaghan *et al.*, 2017) and variability in parameters such as rupture magnitude, rupture velocity, rise time, stress drop, and crustal model (Taborda and Bielak, 2014), among others, should also be progressively included in future versions of Cybershake NZ. In order to increase the comprehensive physics-based simulation limit (i.e., transition frequency) of the results, velocity models with a finer discretization (e.g., 0.2 km) are envisaged for future versions. Epistemic uncertainty in the PSHA results is conventionally addressed by considering alternative GMMs and ERFs using the logic tree approach (Kulkarni, Youngs and Coppersmith, 1984; Reiter, 1991; Bommer *et al.*, 2005), which results in alternative plausible seismic hazard curves for the site of interest. In this context, simulation-based PSHA can be considered as one of the alternative approaches within the considered logic tree branches, as well as using multiple simulation methodologies (as only one of which was considered here). The weight on the simulation-based PSHA can be assigned based on the validity of simulations in different regions of the country (using the detailed analyses conducted to validate simulated ground motions with respect to the observed ground motions).

Acknowledgement

We gratefully acknowledge the support of New Zealand eScience Infrastructure (NeSI) high-performance computing facility, Royal Society of New Zealand, Natural Hazards Research Platform, and QuakeCoRE: The New Zealand Centre for Earthquake Resilience.

References

- Bommer, J. J. *et al.* (2005) 'On the use of logic trees for ground-motion prediction equations in seismic-hazard analysis', *Bulletin of the Seismological Society of America*, 95(2), pp. 377–389.
- Bommer, J. J. *et al.* (2010) 'On the selection of ground-motion prediction equations for seismic hazard analysis', *Seismological Research Letters*, 81(5), pp. 783–793.
- Boore, D. (1983) 'Stochastic simulation of high-frequency ground motions based on seismological models of the radiated spectra', *Bulletin of Seismological Society of America*.
- Bradley, B. A. (2013) 'A New Zealand-Specific Pseudospectral Acceleration Ground-Motion Prediction Equation for Active Shallow Crustal Earthquakes Based on Foreign Models', *Bulletin of the Seismological Society of America*, 103(3), pp. 1801–1822.
- Bradley, B. A. *et al.* (2017) 'Guidance on the utilization of earthquake-induced ground motion simulations in engineering practice', *Earthquake Spectra*. doi: 10.1193/120216EQS219EP.
- Bradley, B. A., Razafindrakoto, H. N. T. and Polak, V. (2017) 'Ground-Motion Observations from the 14 November 2016 M w 7.8 Kaikoura, New Zealand, Earthquake and Insights from Broadband Simulations', *Seismological Research Letters*, 88(3), pp. 740–756.

- Callaghan, S. *et al.* (2017) 'CyberShake: bringing physics-based PSHA to central California. Poster Presentation at 2017 SCEC Annual Meeting. ', *2017 Southern California Earthquake Center Annual Meeting, Poster #303*.
- Campbell, K. W. and Bozorgnia, Y. (2014) 'NGA-West2 ground motion model for the average horizontal components of PGA, PGV, and 5% damped linear acceleration response spectra', *Earthquake Spectra*, 30(3), pp. 1087–1115.
- Eberhart-Phillips, D. *et al.* (2010) 'Establishing a versatile 3-D seismic velocity model for New Zealand', *Seismological Research Letters*, 81(6), pp. 992–1000.
- Foster, K. *et al.* (2019) 'A Vs30 map for New Zealand based on surficial geology, topography, and direct measurements', *Earthquake Spectra*, submitted.
- Goulet, C. A. *et al.* (2015) 'The SCEC broadband platform validation exercise: Methodology for code validation in the context of seismic-hazard analyses', *Seismological Research Letters*, 86(1), pp. 17–26.
- Graves, R. *et al.* (2011) 'CyberShake: A physics-based seismic hazard model for southern California', *Pure and Applied Geophysics*, 168(3–4), pp. 367–381.
- Graves, R. and Pitarka, A. (2010) 'Broadband ground-motion simulation using a hybrid approach', *Bulletin of the Seismological Society of America*, 100(5A), pp. 2095–2123.
- Graves, R. and Pitarka, A. (2015) 'Refinements to the Graves and Pitarka (2010) broadband ground-motion simulation method', *Seismological Research Letters*, 86(1), pp. 75–80.
- King, G. C. P. and Wesnousky, S. G. (2007) 'Scaling of fault parameters for continental strike-slip earthquakes', *Bulletin of the Seismological Society of America*, 97(6), pp. 1833–1840.
- Kulkarni, R. B., Youngs, R. R. and Coppersmith, K. J. (1984) 'Assessment of confidence intervals for results of seismic hazard analysis', in *Proceedings of the Eighth World Conference on Earthquake Engineering*, pp. 263–270.
- Lee, R. L. *et al.* (2017) 'Development of a 3D Velocity Model of the Canterbury, New Zealand, Region for Broadband Ground-Motion Simulation', *Bulletin of the Seismological Society of America*, 107(5), pp. 2131–2150.
- Leonard, M. (2010) 'Earthquake fault scaling: Self-consistent relating of rupture length, width, average displacement, and moment release', *Bulletin of the Seismological Society of America*, 100(5A), pp. 1971–1988.
- Mai, P. M., Spudich, P. and Boatwright, J. (2005) 'Hypocenter locations in finite-source rupture models', *Bulletin of the Seismological Society of America*, 95(3), pp. 965–980.
- Razafindrakoto, H. N. T., Bradley, B. A. and Graves, R. W. (2018) 'Broadband ground-motion simulation of the 2011 Mw 6.2 Christchurch, New Zealand, earthquake', *Bulletin of the Seismological Society of America*. doi: 10.1785/0120170388.
- Reiter, L. (1991) *Earthquake hazard analysis: issues and insights*. Columbia University Press.
- Roten, D. *et al.* (2017) 'Quantification of fault-zone plasticity effects with spontaneous rupture simulations', *Pure and Applied Geophysics*, 174(9), pp. 3369–3391.
- Stirling, M. *et al.* (2012) 'National seismic hazard model for New Zealand: 2010 update', *Bulletin of the Seismological Society of America*, 102(4), pp. 1514–1542.
- Strasser, F. O., Abrahamson, N. A. and Bommer, J. J. (2009) 'Sigma: Issues, insights, and challenges', *Seismological Research Letters*, 80(1), pp. 40–56.
- Taborda, R. *et al.* (2016) 'Evaluation of the southern California seismic velocity models through simulation of recorded events', *Geophysical Journal International*, 205(3), pp. 1342–1364. doi: 10.1093/gji/ggw085.
- Taborda, R. and Bielak, J. (2013) 'Ground-motion simulation and validation of the 2008 Chino Hills, California, earthquake', *Bulletin of the Seismological Society of America*, 103(1), pp. 131–156.
- Taborda, R. and Bielak, J. (2014) 'Ground-motion simulation and validation of the 2008 Chino Hills, California, earthquake using different velocity models', *Bulletin of the Seismological Society of America*.
- Taborda, R., Bielak, J. and Restrepo, D. (2012) 'Earthquake ground-motion simulation including nonlinear soil effects under idealized conditions with application to two case studies', *Seismological Research Letters*, 83(6), pp. 1047–1060.